Mechanism of Strength Evolution of Seawater OPC pastes

Yangyang Zhang, Yanjie Sun, Haibing Zheng,

*Yamei Cai, Wing Lun Lam, Chi Sun Poon**

Department of Civil and Environmental Engineering,
The Hong Kong Polytechnic University,
Hung Hom, Kowloon, Hong Kong, China

*Corresponding author

E-mail: cecspoon@polyu.edu.hk (C.S. Poon)

Abstract: This work investigated the strength degradation mechanisms of seawater ordinary Portland cement (OPC) pastes. Two types of specimens were prepared ((i) OSD sample (i.e., OPC was mixed with seawater, and then cured in deionized (DI) water) and (ii) ODD sample (i.e., OPC was mixed with DI water, and then cured in DI water, as the reference system)). The use of seawater in preparing OPC pastes effectively increased the hydration rate and early-age mechanical strength, but lowered the mechanical strength at the later age. The higher hydration degree and larger amounts of carbonates with a smaller crystal size enabled the seawater OPC pastes to exhibit a higher early-age mechanical strength, increasing by 13.0%-17.0% compared with the DI water OPC pastes. While the formation of Friedel's salt and the formation of calcium-silicate-hydrate (C-S-H) gel with a lower polymerization degree and mean molecular chain length resulted in the deterioration of the pore structure and negatively affected the later-age strength development of the seawater OPC paste, decreasing by 5.8%-11.9% compared with the DI water OPC pastes.

Key words: Seawater; Compressive strength; Cement; Hydration products; Microstructure

1. Introduction

The annul productions of ordinary Portland cement (OPC) and concrete are about 4 billion tonnes and 25 billion tonnes, respectively; and the production of concrete requires huge amounts of fresh water (Xiao et al., 2017; Guo et al., 2020). The World Meteorological Organization estimated that more than half of population worldwide will have difficulties to get enough freshwater (Nishida et al.,2013). Furthermore, the running out of river sand for concrete production is also a major challenge in the construction industry. Desalted sea-sand, as an alternative to river sand, has been

used in concrete production in UK, Japan, South Korea, Turkey and China (Xiao et al., 2017). However, the use of sea-sand can give rise to safety and durability problems due to the presence of salts in the seawater, especially chlorides.

But seawater sea-sand concrete (SSC) is attracting increasing attention worldwide as a novel and environment-friendly construction material that directly uses seawater and sea-sand without desalting (Li et al., 2016; Teng, 2014; Guo et al., 2020; Wang et al., 2018). The active ions (Cl^-, SO_4^{2-}, Mg^{2+} and etc.) of seawater and sea-sand would cause corrosion in steel-reinforced concrete. Generally, seawater and sea-sand can be used in (i) plain concrete, (ii) steel-reinforced concrete where the steel is protected by epoxy resins or other corrosion inhibitors, and (iii) structural concrete that uses fiber reinforced polymer (FRP) in lieu of steel as the reinforcing material (Wang et al., 2018; Yeih et al., 2004; Zheng et al., 2014; Teng, 2014).

Previous works on FRP-SSC mainly focused on its structural behavior and the durability of FRP bars in SSC environment. The mechanical performances of plain pastes/concrete using seawater or sea-sand were also studied in a few studies, but the results were inconsistent (Xiao et al., 2017; Girish et al., 2015; Narver, 1964; Chen et al., 2008; Li et al., 2020; Wang et al., 2018; Chandrakeerthy, 1994; Jau et al., 2006; Islam et al., 2012; Wegian, 2010). Wang et al. (2018), for instance, found that the compressive strength of OPC pastes mixed with seawater can reach to about 53 MPa at 28 days, an increase of 50% compared with DI water OPC pastes. However, Li et al. (2020) observed that the compressive strength of seawater OPC mortars was increased by 15% and 5% at 7 and 14 days, respectively; but the 28-day compressive strength was similar to the DI water OPC mortars. Also, the corresponding flexural strength was decreased by 8% when using seawater, but decreased by 25% when using sea sand. And Chandrakeerthy (1994) also reported that the sea-sand concrete had a similar compressive strength compared with ordinary concrete. However, Grirish et al. (2015) observed that the 28-day compressive strength of sea-sand concrete was lower than that of ordinary concrete. And Kaushik et al. (1995) also found that the compressive strength would be decreased by 13% at 28 days when using seawater. Most studies agreed that seawater

or/and sea-sand concrete had a slightly higher early-age compressive strength but followed by a lower strength development at the later age when compared with ordinary concrete (Xiao et al., 2017; Girish et al., 2015; Narver, 1964; Chen et al., 2008; Jau et al., 2006; Islam et al. 2012; Wegian, 2010). But there have been limited studies that adequately investigate the relationship between mechanical performances and microstructures, especially for the mechanism contributing to the lower strength at the later age.

Thus, this work aimed to provide an in-depth understanding regarding the relationship between the early/late-age compressive strength and hydration characteristics of seawater OPC pastes using different analytical methods.

2. Experimental

2.1. Materials

An ASTM Type 1OPC (ASTM C150M-20, 2020) sourced from Japan and with a specific gravity of 3.15 was used in this work. The chemical compositions of the OPC was characterized by X-ray fluorescence spectroscopy (Supermin200, Rangaku Corporation, Japan) and are shown in Table 1. The mineralogical compositions of the OPC were characterized by X-ray power diffraction and Rietveld refinement analysis (using ICSD database and TOPAS 5.0 software) and the results are as shown in Fig. 1. The result showed that the phase contents of OPC were 70.1 wt.% of C_3S, 10.4 wt.% of C_2S, 8.9 wt.% of C_3A, 7.7 wt.% of C_4AF, and 3.0 wt.% of $C\check{S}H_2$ (gypsum), indicating that this OPC would have a rapid hydration rate and high early-age strength owing to the high content of C_3S. The particle size distribution of OPC was determined using laser diffraction, as shown in Fig. 2. The values of D10, D50 and D90 were 2.34 um, 14.45 um and 35.34 um, respectively. The average particle size (D[4,3]) was 16.95 um. A superplasticizer Glenium SP8S, with a specific gravity of 1.05 and produced by BASF Co. Ltd, was used in this work. The artificial seawater was

prepared according to ASTM D1141-98 (2013), and Table 2 shows the compositions of the artificial seawater.

Table 1 Chemical compositions of OPC (wt%)

CaO	SiO_2	Al_2O_3	Fe_2O_3	SO_3	MgO	K_2O	TiO_2	P_2O_5	ZnO	MnO	CuO	Cl	SrO	ZrO_2
66.10	20.00	5.13	3.24	2.99	1.09	0.60	0.27	0.24	0.10	0.08	0.05	0.04	0.04	0.01

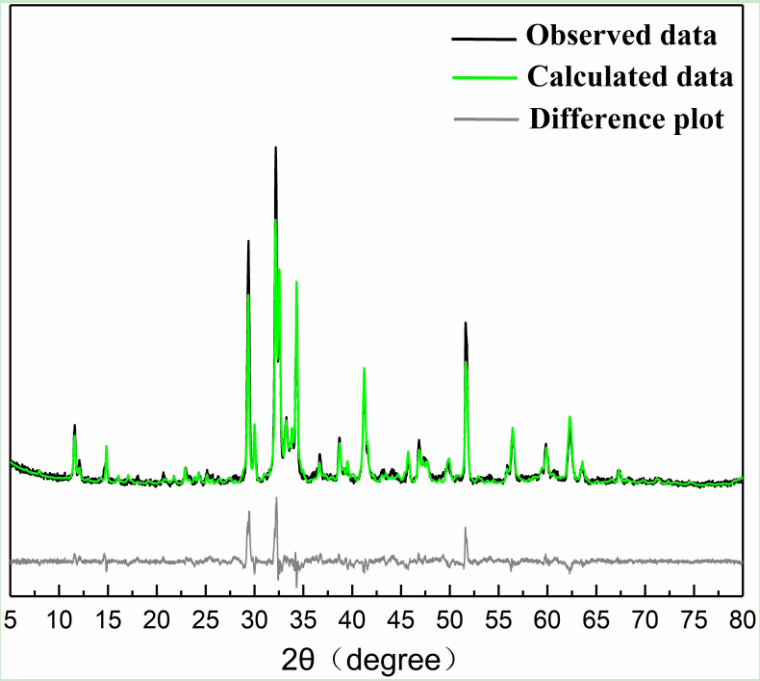

Fig. 1 Rietveld refinement for OPC

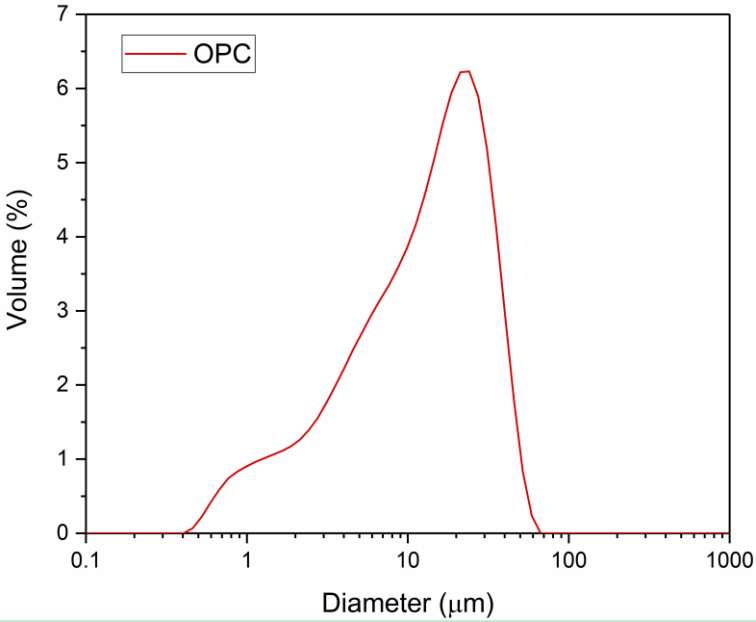

Fig. 2 Particle size distributions of OPC

Table 2 Compositions of the artificial seawater.

Compound	NaCl	$MgCl_2$	Na_2SO_4	$CaCl_2$	KCl	$NaHCO_3$	KBr
Concentration (g/L)	24.53	5.20	4.09	1.16	0.695	0.201	0.101

2.2. Sample preparation

In this work, two types of cement pastes samples were used, i.e., (i) OSD sample, i.e., OPC was mixed with the artificial seawater, and then cured in DI water, which can evaluate the performances of SSC used in inland engineering; and (ii) ODD sample as the reference system used for comparing the macro-performances and microstructure of OSD sample, i.e., OPC was mixed with DI water, and then cured in DI water. DI water was used for avoiding the influence of other ions and clearly investigating the influence of seawater. The water-to-cement (W/C) ratios used in this work were 0.28 (0.5% superplasticizer (SP8S)) and 0.38 (no superplasticizer), which

were designed for evaluating the mechanical properties of concrete with different strength grades. All the cement pastes were prepared at 23 ± 2 °C, cast in the steel cube moulds with size of 40 mm × 40 mm × 40 mm. The samples were placed on a vibrating table for 30 seconds to eliminate entrapped air bubbles. Afterwards, the samples were covered with a plastic wrap, demoulded after 24 hours, and cured in DI water at 23 °C. The curing ages were 1 d, 7 d and 28 d. The compressive strength tests were tested at a loading rate of 0.96 kN/s. The average value of three cubes was taken as the compressive strength. The fractured samples were immersed in isopropanol to stop further hydration. The samples were subsequently used without and with further grinding for the microstructure analysis.

2.3. Characterization methods

The heats of hydration of the cement were acquired using a Calmetrix I-Cal 4000 isothermal calorimeter. The OPC pastes were prepared with W/C ratios of 0.28 and 0.38, mixed with DI water or seawater for 2 minutes prior to the test, and immediately introduced in the calorimeter. The calorimetric data were collected for up to 3 days.

The electrochemical impedance spectroscopy (EIS) test was carried out using a Multi-AutolabM 204 equipment (frequency ranging from 1 Hz to 1 MHz, AC signal magnitude of 10 mV). A two-electrode system was used this work. The impedance spectra were analyzed using a Nova 1.11 software.

X-ray diffraction (XRD) patterns were recorded using a Rigaku Smartlab high-resolution X-ray

diffractometer, operating at 45 kV and 200 mA. The overall data acquisition time per pattern was ~30 minutes in order to obtain a favorable signal-to-noise ratio over the angular range of 5.0°-80.0° 2θ with a 0.020° step size. Rietveld refinement was used for quantifying the mineral compositions using TOPAS 5.0 software. The global refined parameters include background coefficients, zero-shift error, phase scale factors, Lorentz polarization factor, Chebyshev polynomial correction, cell parameters and crystal structures. The ICSD database was used for quantitative analysis, as shown in Table 3.

Table 3 Phases and ICSD codes used for quantitative analysis.

Phase	COD Codes
C_3S	4331
C_2S	81096
C_3A	1841
C_4AF	9197
$C\check{S}H_2$	36186

Thermogravimetric analysis (TGA) was conducted using a Rigaku Thermo Plus EVO2, where about 10 mg of grinded powder was placed in open corundum crucibles and heated from 30°C to 1000°C at a rate of 10°C/min under N_2 atmosphere.

Scanning electron microscopy (SEM) measurements were performed using a Tescan VEGA3 with an accelerating voltage of 20 kV. Energy dispersive spectroscopy (EDS) measurements were also carried out.

^{29}Si magic angle spinning nuclear magnetic resonance (^{29}Si MAS-NMR) spectra were recorded using a GEOL 500 MHz spectrometer using a 7-mm CP/MAS probe (rotation rate of 4500 Hz;

resonance frequency of 79.5 MHz). The ^{29}Si MAS-NMR spectra were recorded with a relaxation delay of 30 seconds and scans of more than 2000.

3. Results and discussion

3.1. Mechanical properties

Fig. 3 shows the mechanical behavior of the hardened OPC pastes using DI water or seawater as the mixing water. The compressive strength results show that the compressive strength was increased with the prolonged curing age and decreased with an increase of W/C, regardless of the type of mixing water used. In addition, the hardened cement pastes using seawater as the mixing water had a higher compressive strength at 1 day when compared with the reference mix, e.g., the compressive strength of the seawater pastes prepared with a W/C ratio of 0.38 was 36.9 MPa, which is an increase of 17.7% compared with DI water pastes; and that with a W/C ratio of 0.28 can reach 42.5 MPa, an increase of 13.0% compared with the corresponding DI water pastes. However, the compressive strength was lower than that of the reference mix starting from 7 days. As an example, the compressive strength of OSD samples at the W/C ratio of 0.38 and 0.28 was 50.5 MPa and 59.9 MPa at 28 days, decreasing by 5.8% and 11.9%, respectively, compared to the corresponding ODD samples. Previous works also reported the evolution of the compressive strength of cement, mortar or concrete, but had inconsistent results (Xiao et al., 2017; Girish et al., 2015; Narver, 1964; Chen et al., 2008; Li et al., 2020; Wang et al., 2018; Chandrakeerthy, 1994; Jau et al., 2006; Islam et al., 2012; Wegian, 2010). A recent work, for instance, exploring the compressive strength of the OPC pastes using seawater as the mixing water and cured in an environmental chamber (20°C and 95% RH), reported that the seawater cement paste showed a higher compressive strength compared with that using DI water as the mixing water, and was increased

by up to 50% after curing for 28 days. Li et al. (2020) observed that the compressive strength of seawater OPC mortars at 28 days was similar to that of DI water OPC mortars. Mbadike et al. (2011) found that using seawater as the mixing water during concrete production would decrease the compressive strength by about 8%. Kaushik et al. (1995) also reported that the usage of seawater can reduce the 28-day compressive strength 13%**.** And most studies agreed that seawater or sea-sand concrete had a higher early-age strength and an inferior long-term (28 days or more) strength than ordinary concrete (Xiao et al., 2017; Girish et al., 2015; Narver, 1964; Chen et al., 2008; Jau et al., 2006; Islam et al. 2012; Wegian, 2010). The main reasons regarding different strength behavior were ascribed to the different mineral compositions of OPC and curing conditions.

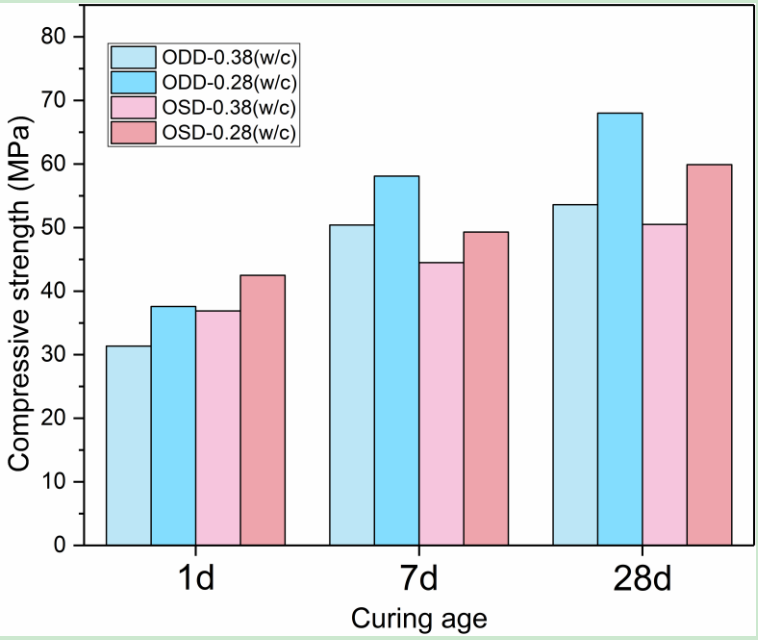

Fig. 3 Compressive strength of seawater OPC pastes

3.2. EIS measurements

Fig. 4 shows the results of electrochemical impedance test of the ODD and OSD samples. The impedance moduli of the hydrated cement samples were related to the pore structures to some extent. It can be seen in Fig. 4 that the impedance moduli of ODD and OSD samples with a W/C of 0.28 was higher than that with a W/C of 0.38 at all curing ages, indicating the denser pore structure and higher compressive strength of the samples prepared with a lower W/C. In addition, the 1-day impedance moduli of the seawater pastes was lower than the DI water pastes although the 1-day compressive strength of OSD was higher compared to ODD sample, which was due to the presence of active ions in the seawater. Furthermore, with respect to the samples prepared with a W/C of 0.38, the impedance moduli of OSD samples decreased by 2.52% (1 day), 3.53% (7 days) and 1.07% (28 days), respectively, compared to ODD samples; but with respect to the samples prepared with a W/C of 0.28, the impedance moduli of OSD samples reduced by 21.97% (1 day), 19.05% (7 days) and 19.63% (28 days), respectively, compared to ODD samples. Thus, a low W/C ratio would significantly decrease the impedance moduli when mixing with seawater, indicating that the corrosion ions in the exterior environment can easily enter into the samples, which further negatively affected the durability.

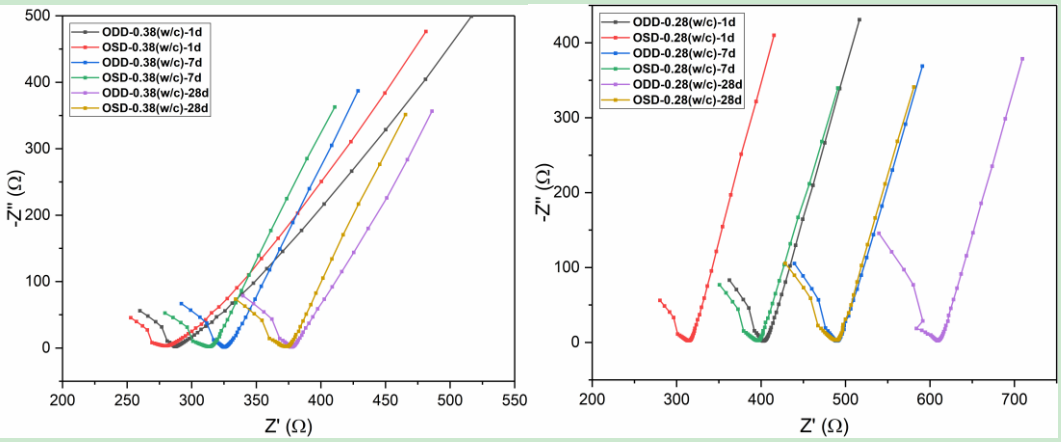

Fig. 4. EIS of ODD and OSD samples prepared with different W/C ratios.

3.3. Hydration heat

Fig. 5 shows the hydration heat results of the different OPC pastes prepared with W/C of 0.38 and 0.28. It can be seen that after the induction period, the exothermic heat signals of the seawater OPC pastes appeared earlier, regardless of the W/C used, indicating that seawater effectively accelerated the hydration rate of OPC pastes owing to the presence of active ions (e.g., Na^{+}, Mg^{2+}, Ca^{2+}, Cl^{-} and SO_4^{2-} ions can effectively accelerate the hydration rate of C_3S (Edwards and Angstadt, 1966)). In addition, different W/C ratios showed different acceleration effects. With respect to ODD-0.38(W/C) sample, the induction period ended and the acceleration period started at 3.4 hours, and with respect to OSD-0.38(W/C) sample, this same period started at 2.5 hours, and thus the use of seawater shortened the induction period by 0.9 hours for the W/C ratio of 0.38. With respect to ODD-0.28(W/C) sample, the induction period ended and the acceleration period started at 3.9 hours, and with respect to OSD-0.28(W/C) sample, this period was at 2.3 hours, and thus the use of seawater shortened the induction period by 1.6 hours when the W/C ratio of 0.28 was used. Thus, the acceleration effect of seawater was more obvious with the use of a lower W/C ratio. Furthermore, the use of seawater increased the amount of hydration heat. The heat flow peaks of the seawater OPC pastes were higher, compared to DI water OPC pastes.

Thus it can conclude that the active ions in seawater effectively (i) promoted the precipitation of the ions formed by OPC minerals; and (ii) combined the ions of dissolved minerals and formed new hydration products (e.g., Cl^{-} would chemically bind with Ca^{2+}, Al^{3+}, and OH^{-} ions to form Friedel's salt), both of which released a higher amount of hydration heat.

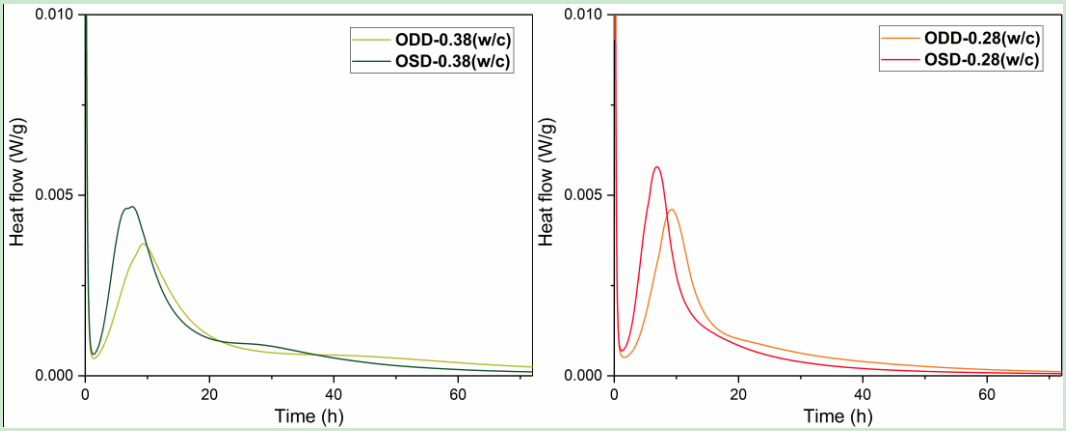

Fig. 5 Hydration heat evolution for pastes prepared with different W/C.

3.4. Phase assemblages

The hydration products of the DI water and seawater OPC pastes were analyzed by XRD and TG-DTG measurements. Fig. 6 shows the XRD results and Fig. 7 shows the corresponding TG-DTG results.

At 1 day of hydration, the main crystalline phases of the DI water pastes were consisted of CH, unreacted C_2S and C_3S (Fig. 6), and an amorphous C-S-H phase was also formed according to the TG-DTG results, as shown in Fig. 7. Apart from the hydration products mentioned above, Friedel's salt ($Ca_4Al_2(OH)_{12}Cl_2 \cdot 4H_2O$), as a new hydration product, was formed in the seawater OPC pastes at 1 day. Previous works also reported the presence of Friedel's salt, which was a characteristic hydration product and formed by the reaction of chloride ion with C_3A and CH or ettringite (AFt) when seawater was used (Wang et al., 2018; Santhanam et al., 2006; Li et al., 2017b; Hirao et al., 2005). And at 7 or 28 days of hydration, the types of hydration products were similar to that at 1 day.

The measured weight loss from 390 to 450°C (normally attribute to the decomposition of CH in the hydrated pastes) at 1 day (Fig. 7) was 2.59 wt.% (ODD-0.28(W/C)), 2.85 wt.% (OSD-0.28(W/C)), 3.56 wt.% (ODD-0.38(W/C)) and 4.06 wt.% (OSD-0.38(W/C)), respectively, indicating that a higher amount of CH was formed with the increased W/C ratio. In addition, the seawater pastes also had a higher amount of CH at 1 day compared to the DI water pastes, regardless of the w/c used, corresponding to the higher hydration degree in the seawater pastes.

Furthermore, the amounts of C-S-H gel formed was also different i.e., the weight loss associated with of C-S-H gel at 1 day increased with using seawater as the mixing water, indicating the higher content of C-S-H gel and hydration degree in the seawater pastes. The amount of carbonate in the DI water pastes and seawater pastes were also different. The measured weight loss from 500 to 700°C in the hydrated pastes at 1 day (Fig. 7) was 2.87 wt.% (ODD-0.28(W/C)), 4.03 wt.% (OSD-0.28(W/C)), 3.64 wt.% (ODD-0.38(W/C)) and 4.86 wt.% (OSD-0.38(W/C)), respectively, indicating that the amount of carbonates in all sections of the seawater pastes was higher than that in the DI water pastes after 1 day of hydration, which was due to (i) the presence of HCO_3^- ion in seawater itself and (ii) the higher solubility of CO_2 in the seawater, compared to DI water.

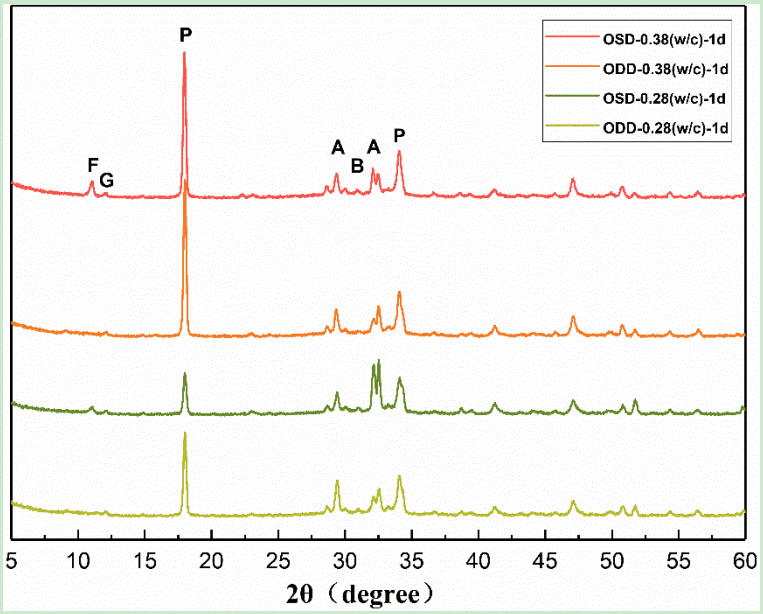
OSD-0.38(w/c)-1d
ODD-0.38(w/c)-1d
OSD-0.28(w/c)-1d
ODD-0.28(w/c)-1d
P
A
A
P
F
G
B
5
10
15
20
25
30
35
40
45
50
55
60
2θ（degree）

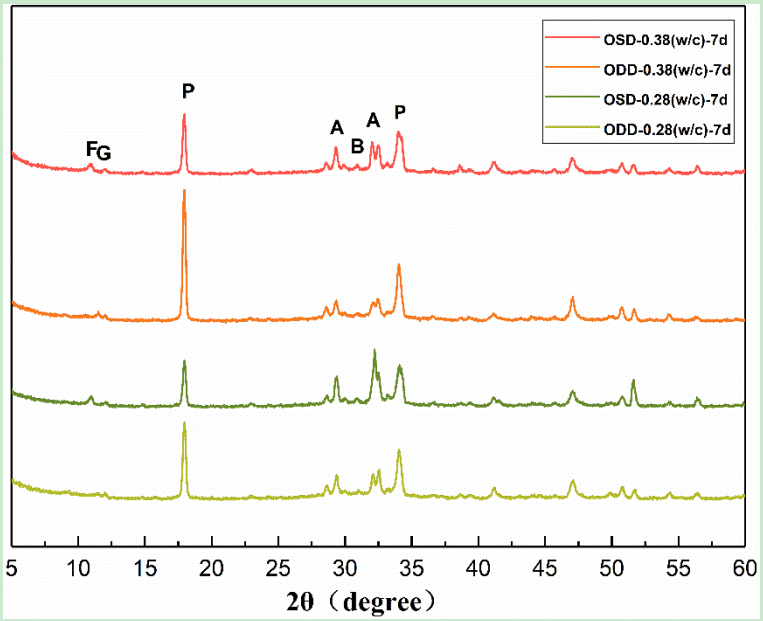
OSD-0.38(w/c)-7d
ODD-0.38(w/c)-7d
OSD-0.28(w/c)-7d
ODD-0.28(w/c)-7d
P
A
A
P
FG
B
5
10
15
20
25
30
35
40
45
50
55
60
2θ（degree）

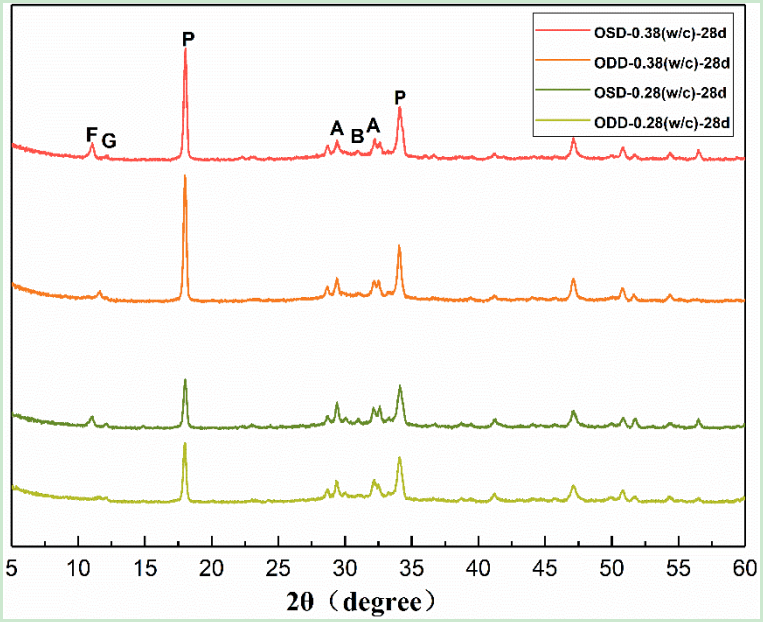

Fig. 6 XRD patterns of DI water and seawater OPC pastes.

Legend: F: Friedel's salt; G: gypsum; P: CH; A: alite (C_3S); B: belite (C_2S).

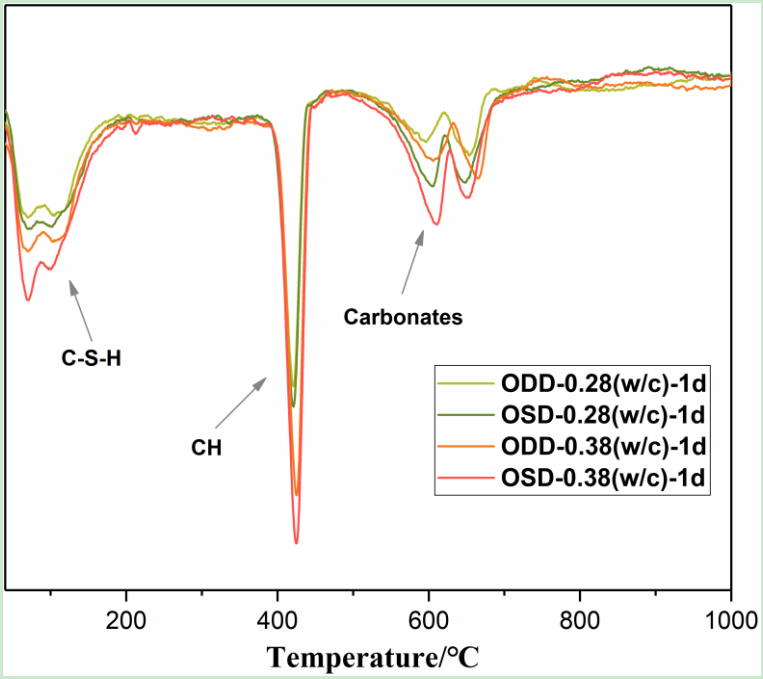

Fig. 7 TG-DTG curves of DI water and seawater OPC pastes at 1 day

3.5. Relation between compressive strength and hydration product evolution

The compressive strength of a cementitious material is significantly related to its hydration

product evolution. For the early-age strength of the seawater pastes , as shown in Fig. 7, the larger amount of CH in the seawater OPC pastes indicated that seawater can effectively accelerate the hydration rate of OPC pastes owing to the presence of active ions (Cl^-, Na^+, Mg^{2+}, Ca^{2+}, SO_4^{2-}) in seawater (Wilding et al., 1984). Thus, the seawater pastes would show a denser pore structure and a higher compressive strength compared with the DI water pastes at early age. In addition, the formation of small-sized or poorly-crystalline carbonates might also contribute to the development of the early-age strength of the seawater pastes. It can be seen in Fig. 7 that a larger amount of carbonates was formed in the seawater pastes at 1 day compared with the DI water pastes. But, the decomposition temperature of the carbonates in the seawater pastes was significantly lower than that measured in the DI water pastes, indicating that the crystal size of the carbonates formed in the seawater OPC pastes was smaller than that formed in the DI water pastes. And the smaller sized carbonates would normally exhibit a high hardness and mechanical strength (Hu et al., 2010). Furthermore, the freshly formed carbonated with a smaller crystal size would also grow, leading to the interlocking among the carbonates (Wang et al., 2019a), as also shown in Fig. 10, both of which can contribute to the compressive strength.

On the other hand, two main factors negatively impacted the development of compressive strength of the seawater OPC pastes at 7 and 28 days. Firstly, the formation of Friedel's salt negatively affected the mechanical strength of the OSD sample. The crystal structure of Friedel's salt is composed of positively charged main layers containing 12 hydroxyl groups (i.e., $[Ca_4Al_2(OH)_{12}]^{2+}$) and the negatively charged interlayers comprising 4 H_2O molecules (i.e., $[2Cl^-, 4H_2O]$) (Grishchenko et al., 2013). Friedel's salt is a member of the aluminate-ferrite-monosubstituent

(AFm) family having the general formula $[Ca_2(Al,Fe)(OH)_6]\cdot X\cdot xH_2O$ where X is a monovalent ion (i.e., OH^-, Cl^-, or $[AlSi(OH)_8]^-$) or half of a divalent interlayer anion (i.e. SO_4^{2-} or CO_3^{2-}), and x is the number of H_2O molecules (Taylor, 1997; Bizzozero, 2014). Friedel's salt, as a chloride-containing AFm phase, can be formed by the chemical reaction between chloride and some AFm phases like monosulfoaluminate, monocarboaluminate and hemicarboaluminate (Sui et al., 2019). In addition, AFm phases also belong to the lamellar double hydroxide family exhibiting typical hexagonal platelets morphology, and previous works also confirmed that Friedel's salt crystallizes in a hexagonal manner with a particle size of several microns (Birnin-Yauri and Glasser, 1998; Talero and Trusilewicz, 2012; Li et al., 2017a). This large-size and hexagon-like Friedel's salt crystals might have a lower hardness, and grow with a higher porosity, as shown in Fig. 10.

Secondly, the changes in the structure of C-S-H gel also had an influence on the strength development of the OSD sample. ^{29}Si MAS-NMR measurements were used to investigate the structure of C-S-H gel formed during the hydration of ODD and OSD samples, and Fig. 8 shows the ^{29}Si MAS-NMR spectra of ODD and OSD pastes at 28 days. Generally, the ^{29}Si MAS-NMR spectra in the OPC pastes shows different signals of Q^n structural units, approximately (i) -68 to -75 ppm corresponding to the Q^0, (ii) -76 to -82 ppm corresponding to the Q^1, (iii) -82 to -88 ppm corresponding to the Q^2, (iv) -88 to -98 ppm corresponding to the Q^3, and (v) -98 to -120 ppm (; Wang et al., 2019a; Wang et al. 2019b; Da Silva Andrade et al., 2019).

It is observed in Fig. 8 that after OPC was hydrated with DI water or seawater, the cement pastes exhibited two silicate groups, Q1 and Q2, indicating that C-S-H gel was formed. Peakfit 4.12

software was used to calculate the ratio of Q0, Q1 and Q2 resonances. And the polymerization degree (PD = Q2/Q1. (Wang et al. 2019b)) of C-S-H in ODD and OSD sample was 0.598 and 0.567, respectively; and the mean molecular chain length (MCL=2(Q1+Q2)/Q1. (Wang et al., 2019a; Wang et al. 2019b)) of C-S-H in ODD and OSD sample was 3.20 and 3.13, respectively, indicating the structure of C-S-H gel in the two hydrated pastes varied obviously, i.e., the polymerization degree and mean molecular chain length of C-S-H gel in the OSD sample were lower than that in the ODD sample. Thus, the polymerization degree and mean molecular chain length of C-S-H gel decreased when OPC was mixed with seawater instead of DI water. The active ions of seawater were closely related to the change of C-S-H gel.

SEM-EDS measurements were carried out to investigate the composition of C-S-H gel, as shown in Fig. 9. It can be seen in Fig. 9 that C-S-H gel formed in the ODD and OSD samples displayed a disordered network morphology. However, the composition of C-S-H gel in the two pastes was different, i.e., traces of chloride and sodium were detected in the structure of C-S-H gel in the OSD sample according to the EDS results. Previous works also found the chloride binding in the C-S-H gel (De Weerdt et al., 2015; Shi et al., 2017; Beaudoin et al., 1990; Florea and Brouwers, 2012). De Weerdt et al. (2015), for instance, exploring the impact of cation on chloride binding of C-S-H gel, reported that the chloride binding of C-S-H gel contributed substantially to the total amount of chloride binding in OPC pastes, and the content of chloride increased when the OPC paste was exposed to $MgCl_2$ and $CaCl_2$ solution instead of NaCl solution. In this work, NaCl, $MgCl_2$ and $CaCl_2$ were all present in seawater, and thus chloride can be easily detected in the structure of C-S-H gel. In addition, Lothenbach et al. (2015) reported that sodium could replace calcium and

be present in the interlayer space of C-S-H, leading to a decrease of the mean molecular chain length of C-S-H gel. This is further confirmed in this work (i.e., the EDS and ^{29}Si MAS-NMR data), and the change of C-S-H structure would result in the decrease of bonding ability and cross-linking degree, and reduce the bearing capacity of specimens when suffering from the external load, and therefore negatively affecting the strength development of the OSD sample, as simplified in Fig. 10.

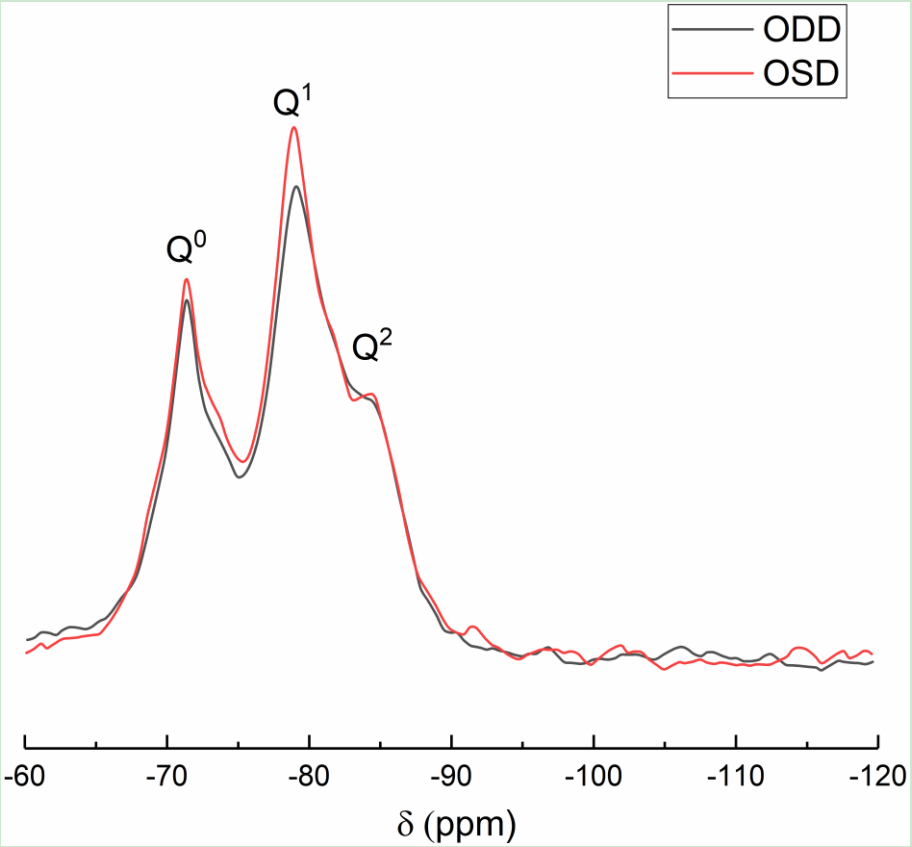

Fig. 8 ^{29}Si MAS-NMR spectra of ODD and OSD pastes.

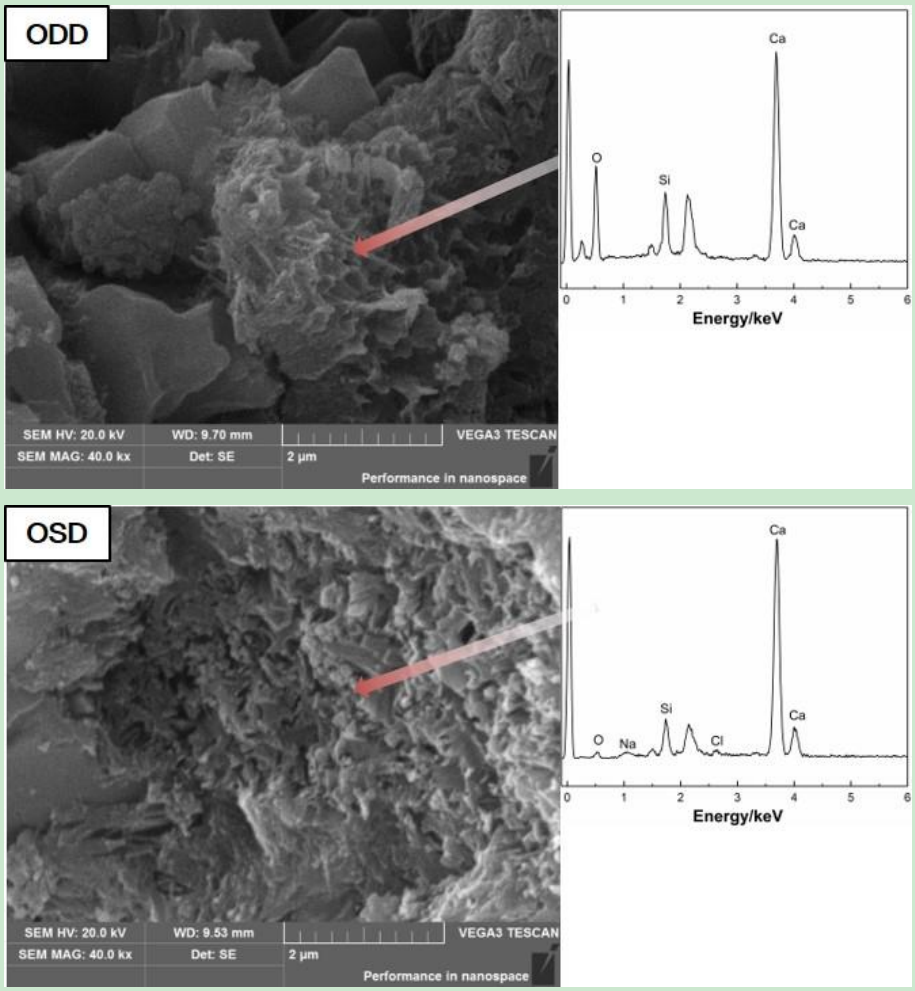

Fig. 9 SEM-EDS data of C-S-H gel present in the ODD and OSD pastes

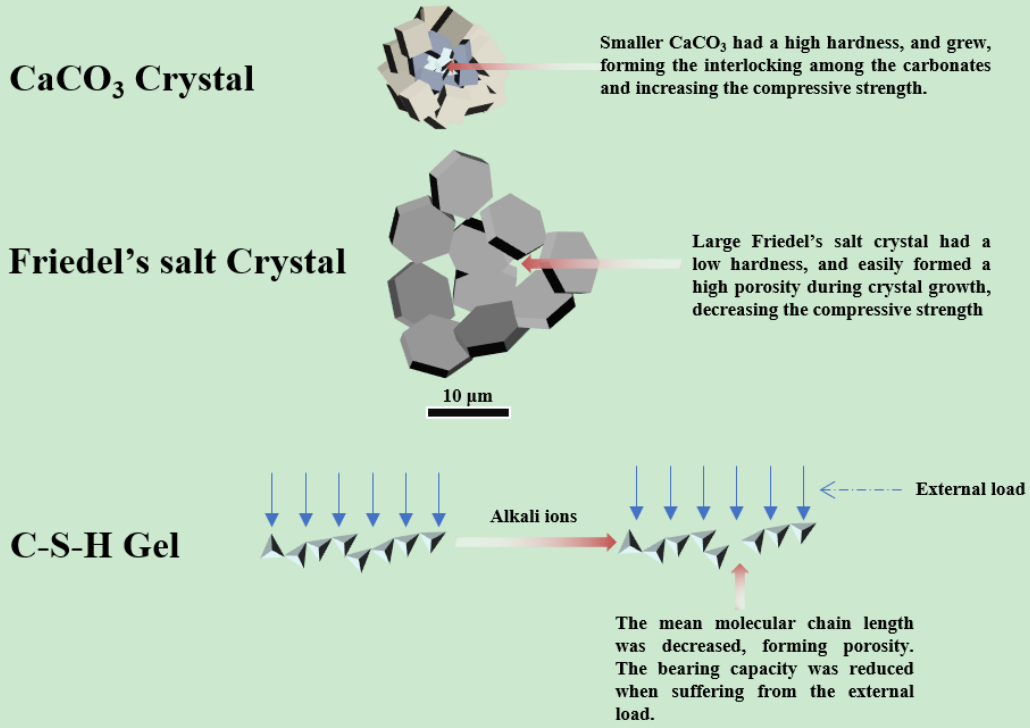

Fig. 10 Schematic diagram of the relation between compressive strength and hydration product evolution

4. Conclusion

In this work, the strength degradation mechanisms of seawater OPC pastes were investigated using different characterization methods. The use of seawater can effectively increase the hydration rate and early-age mechanical strength of the OPC pastes. However, compared with DI water OPC pastes, some decrease in strength occurred starting at about 7 days of hydration. The high early-age mechanical strength of the seawater OPC pastes was closely related to its microstructure. The amount of CH in the seawater OPC pastes was higher than that of the DI water OPC pastes, indicating the acceleration effect of using seawater, and thus the early-age seawater OPC pastes would have a denser pore structure. In addition, compared with the DI water OPC pastes, a larger amount of carbonates was formed in the seawater OPC paste at 1 day. The smaller crystal size of the carbonates would effectively contribute to the mechanical strength of the seawater OPC pastes. Regarding the seawater OPC pastes at 7 or 28 days, two main factors would negatively affect its strength development. Firstly, the formation of Friedel's salts with a large size in the seawater OPC pastes led to the deterioration of the pore structure. Secondly, the

polymerization degree and mean molecular chain length of C-S-H gel decreased, negatively affecting the bonding ability and cross-linking degree, and therefore lowered the strength.

Acknowledgments

The authors wish to thank the financial supports of the Research Grants Council Theme Based Research Scheme and the Hong Kong Polytechnic University. We gratefully acknowledge the support of the University Research Facility on Chemical and Environmental Analysis (UCEA) of PolyU.

References:

ASTM. C150M-20 (2020) Standard Specification for Portland Cement.

Beaudoin JJ, Ramachandran VS and Feldman RF (1990) Interaction of chloride and C-S-H. *Cement and Concrete Research* 20: 875-883.

Birnin-Yauri UA and Glasser FP (1998) Friedel's salt, $Ca_2Al(OH)_6(Cl,OH)\cdot 2H_2O$: its solid solutions and their role in chloride binding. *Cement and Concrete Research* 28: 1713-1723.

Bizzozero J (2014) *Hydration and dimensional stability of calcium aluminate cement based systems*. PhD Thesis, Swiss federal Institute of Technology in Lausanne, Switzerland.

Chandrakeerthy SR (1994) Suitability of sea sand as a fine aggregate for concrete production. *Transactions, Institution of Engineers* 93-114.

Chen ZL, Tang XN, Sun GF, et al. (2008) Research on durability and application of seawater concrete. *Ocean Engineering* 26: 102-106.

Da Silva Andrade D, Da Silva Rêgo JH, Morais PC, et al. (2019) Investigation of C-S-H in ternary cement pastes containing nanosilica and highly-reactive supplementary cementitious materials (SCMs): Microstructure and strength. *Construction and Building Materials* 198: 445-455.

De Weerdt K, Colombo A, Coppola L, et al. (2015) Impact of the associated cation on chloride binding of Portland cement paste. *Cement and Concrete Research* 68: 196-202.

Edwards GC and Angstadt RL. (1966) The effect of some soluble inorganic admixtures on the early hydration of portland cement. *Journal of Applied Chemistry* 16: 166-168.

Florea MVA and Brouwers HJH. (2012) Chloride binding related to hydration products. *Cement and Concrete Research* 42: 282-290.

Girish CG, Tensing D and Priya K. (2015) Dredged offshore sand as a replacement for fine aggregate in concrete. *International Journal of Engineering Sciences & Emerging Technologies* 8: 88-95.

Grishchenko RO, Emelina AL and Makarov PY. (2013) Thermodynamic properties and thermal behavior of Friedel's salt. *Thermochimica Acta* 570: 74-79.

Guo M, Hu B, Xing F, et al. (2020) Characterization of the mechanical properties of eco-friendly

concrete made with untreated sea sand and seawater based on statistical analysis. *Construction and Building Materials* 234: 117339.

Hirao H, Yamada K, Takahashi H, et al. (2005) Chloride binding of cement estimated by binding isotherms of hydrates. *Journal of Advanced Concrete Technology* 3: 77-84.

Hu G, Cai X and Rong Y (2010) *Fundamentals of Material Science*. Shanghai Jiaotong University Press, Shanghai.

Islam MM, Islam MS, Al-Amin M, et al. (2012) Suitability of sea water on curing and compressive strength of structural concrete. *Journal of Civil Engineering (the Institution of Engineers, Bangladesh)* 40 (1) 37-45.

Jau W, Tan J and Yang C (2006) Effect of sea sand on concrete durability and its management. *Journal of Southeast University (Natural Science Edition)* 36 (supplement) 160-166S2.

Kaushik SK and Islam S. (1995) Suitability of sea water for mixing structural concrete exposed to a marine environment. *Cement and Concrete Composites* 17: 177-185.

Li D, Guo X, Tian Q, et al. (2017a) Synthesis and application of Friedel's salt in arsenic removal from caustic solution. *Chemical Engineering Journal* 323: 304-311.

Li G, Zhang A, Song Z, et al. (2017b) Study on the resistance to seawater corrosion of the cementitious systems containing ordinary Portland cement or/and calcium aluminate cement. *Construction and Building Materials* 157: 852-859.

Li P, Li W, Yu T, et al. (2020) Investigation on early-age hydration, mechanical properties and microstructure of seawater sea sand cement mortar. *Construction and Building Materials* 249: 118776.

Li YL, Zhao XL, Singh RKR, et al. (2016) Experimental study on seawater and sea sand concrete filled GFRP and stainless steel tubular stub columns. *Thin-Walled Structures* 106: 390-406.

Lothenbach B and Nonat A. (2015) Calcium silicate hydrates: Solid and liquid phase composition. *Cement and Concrete Research* 78: 57-70.

Mbadike EM and Elinwa AU (2011) Effect of salt water in the production of concrete. *Nigerian Journal of Technology* 30: 105-110.

Narver DL. (1964) Good concrete made with coral and water. *Civil Engineering* 24: 654-658.

Nishida T, Otsuki N, Ohara H, et al. (2013) Some considerations for applicability of seawater as mixing water in concrete. *Journal of Materials in Civil Engineering* 27: B4014004.

Santhanam M, Cohen M and Olek J. (2006) Differentiating seawater and groundwater sulfate attack in Portland cement mortars. *Cement and Concrete Research* 36: 2132-2137.

Shi Z, Geiker MR, De Weerdt K, et al. (2017) Role of calcium on chloride binding in hydrated Portland cement-metakaolin-limestone blends. *Cement and Concrete Research* 95: 205-216.

Sui S, Wilson W, Georget F, et al. (2019) Quantification methods for chloride binding in Portland cement and limestone systems. *Cement and Concrete Research* 125: 105864.

Talero R and Trusilewicz L. (2012) Morphological differentiation and crystal growth form of Friedel’s salt originated from pozzolan and Portland cement. *Industrial & Engineering Chemistry Research* 51: 12517-12529.

Taylor H F W (1997) *Cement chemistry*. Thomas Telford.

Teng JG. (2014) Performance enhancement of structures through the use of fibrereinforced polymer (FRP) composites, In: *Proceedings of 23rd Australasian Conference on the Mechanics of Structures and Materials (ACMSM23)*, keynote presentation, Lismore, Australia.

Wang D, Fang Y, Zhang Y, et al. (2019a) Changes in mineral composition, growth of calcite crystal,

and promotion of physico-chemical properties induced by carbonation of β-C2S. *Journal of CO_2 Utilization* 34: 149-162.

Wang J, Liu E and Li L. (2018) Multiscale investigations on hydration mechanisms in seawater OPC paste. *Construction and Building Materials* 191: 891-903.

Wang J, Han B, Li Z, et al. (2019b) Effect investigation of nanofillers on CSH gel structure with Si NMR. *Journal of Materials in Civil Engineering* 31(1): 04018352.

Wegian FM (2010) Effect of seawater for mixing and curing on structural concrete. *The IES Journal Part A: Civil & Structural Engineering* 3 (4) 235-243.

Wilding CR, Walter A and Double DD. (1984) A classification of inorganic and organic admixtures by conduction calorimetry. *Cement and Concrete Research* 14: 185-194.

Xiao J, Qiang C, Nanni A, et al. (2017) Use of sea-sand and seawater in concrete construction: Current status and future opportunities. *Construction and Building Materials* 155: 1101-1111.

Yeih W, Chang JJ and Tsai CL. (2004) Enhancement of the bond strength of epoxy coated steel by the addition of fly ash. *Cement and Concrete Composites* 26: 315-321.

Zheng H, Li W, Ma F, et al. (2014) The performance of a surface-applied corrosion inhibitor for the carbon steel in saturated $Ca(OH)_2$ solutions. *Construction and Building Materials* 55: 102-108.